

# Electrochemical determination of thermodynamic properties of saturated solid solutions of $\text{Hg}_2\text{GeSe}_3$ , $\text{Hg}_2\text{GeSe}_4$ , $\text{Ag}_2\text{Hg}_3\text{GeSe}_6$ , and $\text{Ag}_{1.4}\text{Hg}_{1.3}\text{GeSe}_6$ compounds in the Ag–Hg–Ge–Se system

M.V. Moroz<sup>1</sup> · M.V. Prokhorenko<sup>2</sup> · O.V. Reshetnyak<sup>3</sup> · P.Yu. Demchenko<sup>4</sup>

Received: 25 March 2016 / Revised: 30 September 2016 / Accepted: 3 October 2016 / Published online: 18 October 2016  
© Springer-Verlag Berlin Heidelberg 2016

**Abstract** Triangulation of the Ag–Hg–Ge–Se system in the vicinity of  $\text{GeSe}_2$ ,  $\text{HgSe}$ ,  $\text{Hg}_2\text{GeSe}_3$ ,  $\text{Hg}_2\text{GeSe}_4$ ,  $\text{Ag}_2\text{Hg}_3\text{GeSe}_6$ , and  $\text{Ag}_{1.4}\text{Hg}_{1.3}\text{GeSe}_6$  compounds and selenium was performed using X-ray diffraction and differential thermal analysis methods. The spatial position of the determined four-phase regions regarding figurative point of silver was used to write the equations of virtual potential-forming chemical reactions. Potential-forming processes were performed in electrochemical cells (ECCs) of the type  $(-)\text{C} | \text{Ag} | \text{Ag}_3\text{GeS}_3\text{I glass} | \text{D} | \text{C} (+)$  where C are the inert (graphite) electrodes, Ag and D are the electrodes of the ECCs, D represents equilibrium four-phase alloys, and  $\text{Ag}_3\text{GeS}_3\text{I}$  glass is a membrane with purely ionic  $\text{Ag}^+$  conductivity. The linear dependences of the EMF of galvanic cells on temperature in the range of 425–455 K were used to calculate the standard thermodynamic values of saturated solid solutions of  $\text{Hg}_2\text{GeSe}_3$ ,  $\text{Hg}_2\text{GeSe}_4$ ,  $\text{Ag}_2\text{Hg}_3\text{GeSe}_6$ , and  $\text{Ag}_{1.4}\text{Hg}_{1.3}\text{GeSe}_6$  compounds.

**Keywords** Ag–Hg–Ge–Se system · Phase equilibria · Thermodynamic properties · EMF method

✉ M.V. Moroz  
riv018@i.ua

<sup>1</sup> Department of Chemistry and Physics, National University of Water and Environmental Engineering, 11, Soborna St, Rivne 33028, Ukraine

<sup>2</sup> Department of Cartography and Geospatial Modeling, Lviv Polytechnic National University, 12, S. Bandery St, Lviv 79013, Ukraine

<sup>3</sup> Department of Physical and Colloid Chemistry, Ivan Franko National University of Lviv, 6 Kyryla i Mefodiya St, Lviv 79005, Ukraine

<sup>4</sup> Department of Inorganic Chemistry, Ivan Franko National University of Lviv, 6 Kyryla i Mefodiya St, Lviv 79005, Ukraine

## Introduction

The phase space of the Ag–Hg–Ge–Se system features the existence of such chalcogenide compounds as  $\text{Ag}_2\text{Se}$  [1],  $\text{GeSe}$ ,  $\text{GeSe}_2$  [2],  $\text{Ag}_2\text{GeSe}_3$  [3],  $\text{Ag}_8\text{GeSe}_6$  [4, 5], and  $\text{HgSe}$ ,  $\text{Hg}_2\text{GeSe}_3$ ,  $\text{Hg}_2\text{GeSe}_4$  [6, 7], as well as four-element phases of variable composition  $\text{Ag}_{\sim 7.12}\text{Hg}_{\sim 6.32}\text{Ge}_{\sim 0.44}\text{Se}_{\sim 0.82}$  ( $\beta$ ),  $\text{Ag}_{\sim 6.08}\text{Hg}_{\sim 4.00}\text{Ge}_{\sim 0.96}\text{Se}_{\sim 2.00}$  ( $\gamma$ ),  $\text{Ag}_{3.4}\text{Hg}_{2.3}\text{GeSe}_6$  ( $\delta$ ),  $\text{Ag}_{\sim 2.24}\text{Hg}_{\sim 2.00}\text{Ge}_{\sim 2.88}\text{Se}_{\sim 3.00}$  ( $\epsilon$ ), and  $\text{Ag}_{1.4}\text{Hg}_{1.3}\text{GeSe}_6$  [8]. Figurative points of most compounds and their solid solutions belong to the Hg–Ge–Se [7] and  $\text{Ag}_2\text{Se}$ – $\text{GeSe}_2$ – $\text{HgSe}$  [8] planes of Gibbs tetrahedron of the Ag–Hg–Ge–Se system. Two-phase alloys in the concentration plane Hg–Ge–Se at  $T \leq 600$  K are found at the sections  $\text{Hg}_2\text{GeSe}_4$ – $\text{GeSe}_2$ ,  $\text{Hg}_2\text{GeSe}_4$ – $\text{HgSe}$ ,  $\text{Hg}_2\text{GeSe}_4$ – $\text{Se}$ ,  $\text{Hg}_2\text{GeSe}_4$ – $\text{HgGeSe}_3$ ,  $\text{Hg}_2\text{GeSe}_3$ – $\text{HgSe}$ ,  $\text{Hg}_2\text{GeSe}_3$ – $\text{GeSe}$ , and  $\text{Hg}_2\text{GeSe}_3$ – $\text{GeSe}_2$  [7]. Two-phase equilibria in the  $\text{Ag}_2\text{Se}$ – $\text{GeSe}_2$ – $\text{HgSe}$  plane are the sections  $\text{Ag}_2\text{Hg}_3\text{GeSe}_6$ – $\text{Hg}_2\text{GeSe}_6$ ,  $\text{Ag}_2\text{Hg}_3\text{GeSe}_6$ – $\text{Ag}_{1.4}\text{Hg}_{1.3}\text{GeSe}_6$ ,  $\text{Ag}_2\text{HgGeSe}_6$ – $\text{HgSe}$ ,  $\text{Ag}_{1.4}\text{Hg}_{1.3}\text{GeSe}_6$ – $\text{GeSe}_2$ , and  $\text{Ag}_{1.4}\text{Hg}_{1.3}\text{GeSe}_6$ – $\text{Hg}_2\text{GeSe}_4$  [8].  $\text{Hg}_2\text{GeSe}_3$  melts incongruently at  $841 \pm 5$  K and has a polymorphous transformation at 810 K [6]. The homogeneity region of  $\text{Hg}_2\text{GeSe}_3$  at 780 K lies within the range of 63.0–66.7 mol% HgSe. The solid solubility of HgSe in  $\alpha$ - and  $\beta$ -phases of GeSe reaches 1 and 28 mol%, respectively. The solid solubility of GeSe in HgSe is negligible [7]. The crystal structure of  $\text{Hg}_2\text{GeSe}_4$  based on powder diffraction data was reported in [8]. Re-investigation of  $\text{Hg}_2\text{GeSe}_4$  based on single-crystal data was performed by Dong Y. et al. [9]. Details about four-element  $T$ – $x$  diagrams of the Ag–Hg–Ge–Se system are limited by the melting point of  $\gamma$ -phase of  $\text{Ag}_6\text{HgGeSe}_6$  composition at 1220 K [10]. The thermodynamic properties of silver selenide [11, 12], germanium mono- and dichalcogenide saturated in silver [13], and  $\text{Ag}_2\text{GeSe}_3$  and  $\text{Ag}_8\text{GeSe}_6$  compounds [13, 14] were

measured by EMF techniques. Thermodynamic properties of stoichiometric HgSe are given in [15].

This paper presents the results of the investigation by EMF method of the thermodynamic properties of silver-saturated  $\text{Hg}_2\text{GeSe}_3$ ,  $\text{Hg}_2\text{GeSe}_4$ , and  $\text{Ag}_{1.4}\text{Hg}_{1.3}\text{GeSe}_6$  compounds and  $\varepsilon$ -phase, i.e.,  $\text{Ag}_2\text{Hg}_3\text{GeSe}_6$ , that is in equilibrium with selenium. The investigation method for assessing the thermodynamic properties was chosen due to the spatial position of the figurative points of the mentioned phases in regard to the points of selenium and silver, and the availability of data on the thermodynamic properties of the HgSe compound [15] as well as the  $\text{GeSe}_2$  phase saturated by silver [13]. Thermodynamic properties of ternary and quaternary phases can be used for analytic modeling of  $p$ - $T$ - $x$  diagrams of the Ag–Hg–Ge–Se system by CALPHAD methods [16, 17].

## Experimental

The crystalline and glassy alloys were synthesized from pure elements (Ag 99.999 wt%, Alfa-Aesar, Germany; Ge 99.9999 wt%, Lenreactiv, Russia; Se 99.999 wt%, Lenreactiv, Russia) and previously prepared HgSe of at least 99.99 wt% purity in quartz ampoules evacuated to 1 Pa according to the procedure described in [18]. The mass of the synthesized alloys was 5 g. The maximum synthesis temperature of the crystalline alloys was 1050 K. Glassy  $\text{Ag}_3\text{GeS}_3\text{I}$  [19] was obtained by melt quenching from 1200 K into ice water. The alloys for the positive electrodes of electrochemical cells (ECCs) were ground to particle size of  $\leq 5 \mu\text{m}$  and homogenized by annealing at 600 K for 48 h. The phase composition of the alloys was determined by X-ray diffraction (XRD) and differential thermal analysis (DTA) methods. DTA experiments were performed in evacuated quartz ampoules ( $p \leq 1 \text{ Pa}$ ). The DTA curves of alloys were recorded using a Paulik-Paulik-Erdey derivatograph (Hungary) fitted with chromel-alumel thermocouples and an H307-1 XY recorder (Ukraine). The thermocouples were calibrated by the melting points of In (429 K), Sn (505 K), Cd (594 K), Te (723 K), Sb (904 K), NaCl (1074 K), Ge (1209 K), Ag (1236 K), and Cu (1357 K) [20]. The heating (cooling) rate of the DTA scans was  $6\text{--}8 \text{ K min}^{-1}$ . The temperature measurement error did not exceed  $\pm 5 \text{ K}$ . XRD patterns were collected on a STOE STADI P diffractometer (Germany) equipped with a linear position-sensitive detector, in a modified Guinier geometry (transmission mode,  $\text{CuK}\alpha_1$  radiation, a bent Ge (111) monochromator,  $2\theta/\omega$  scan mode). XRD data sets were processed using STOE WinX<sup>POW</sup> (version 2.21) [21] and PowderCell (version 2.3) [22] software suits.

Potential-forming processes were performed in electrochemical cells of the type (–) C | Ag |  $\text{Ag}_3\text{GeS}_3\text{I}$  glass | D | C (+) where C are the inert graphite electrodes; Ag and D are the electrodes of ECCs; D represents equilibrium four-phase alloys, and  $\text{Ag}_3\text{GeS}_3\text{I}$  glass is a membrane with purely ionic

$\text{Ag}^+$  conductivity [19].  $\text{Ag}_3\text{GeS}_3\text{I}$  glass, same as  $\text{Ag}_3\text{GeS}_3\text{Br}$  [23], belongs to the class of superionic materials [24]. The equilibrium in ECCs ( $E = \text{const}$ ) was achieved during 4–6 h. The equilibria were considered when the EMF values were constant or their variations did not exceed  $\pm 0.2 \text{ mV}$ .

Powdered cell components were pressed at  $10^8 \text{ Pa}$  through the holes of 2-mm diameter arranged in the PTFE matrix up to density  $\rho = (0.93 \pm 0.02)\rho_0$ , where  $\rho_0$  is the experimentally determined density of cast alloys. To eliminate the possible defects of plastic deformation during the pressing of alloys, we performed five-fold thermal cycling of ECCs in the range of 400–480 K with heating and cooling rates of  $2 \text{ K min}^{-1}$ . The ECCs were heated in a resistance furnace similar to that described in [25] filled with a mixture of  $\text{H}_2$  and Ar (both supplied by Lviv chemical factory, Ukraine, 0.9999 volume fraction) in a molar ratio of 1:9,  $p = 1.2 \times 10^5 \text{ Pa}$ . Spectrally pure hydrogen was obtained by the diffusion of the bottled gas through palladium foil. The flow of argon was purified from oxygen in a quartz tube by copper foil heated to 673 K. The flow of gas at the rate of  $2 \cdot 10^{-3} \text{ m}^3 \text{ h}^{-1}$  had the direction from the positive to the negative electrodes of the ECCs. The temperature was maintained with an accuracy of  $\pm 0.5 \text{ K}$ . The EMF values of the cells were measured using the voltmeter of a U7–9 electrometric amplifier (Ukraine) with an input resistance of  $>10^{12} \Omega$ . The temperature dependences  $E(T)$  of the EMF of the cells were analyzed according to the technique in [26].

## Results and discussion

The lines of two-phase alloys in Fig. 1 marked out four-phase regions  $\text{Hg}_2\text{GeSe}_4$ –Se–HgSe– $\text{Ag}_2\text{Hg}_3\text{GeSe}_6$  (I),  $\text{Hg}_2\text{GeSe}_4$ –

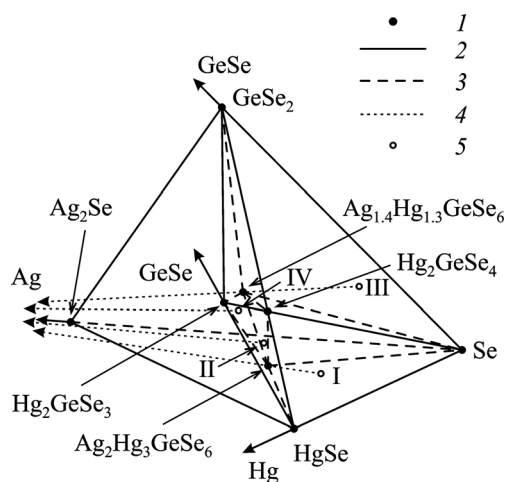


**Fig. 1** Four-phase regions of the Ag–Hg–Ge–Se system in the  $\text{GeSe}_2$ –HgSe– $\text{Hg}_2\text{GeSe}_3$ – $\text{Hg}_2\text{GeSe}_4$ – $\text{Ag}_{1.4}\text{Hg}_{1.3}\text{GeSe}_6$ – $\text{Ag}_2\text{Hg}_3\text{GeSe}_6$ –Se phase region below 600 K: 1—figurative points of compounds and their saturated solid solutions; 2, 3—lines of two-phase equilibria; 4—sections of the concentration space connecting the figurative points of silver and positive electrodes D of ECCs; 5—figurative points of alloys of positive electrodes of ECCs of the phase regions (I)–(IV)

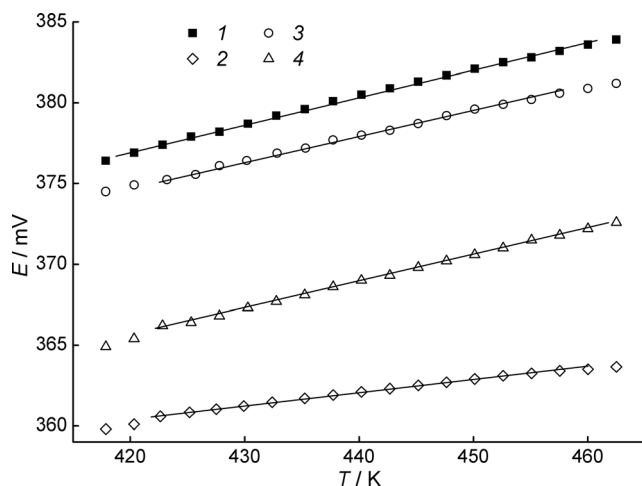
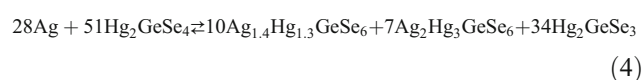
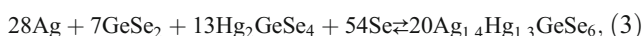


**Fig. 2** The dependences of EMF ( $E$ ) vs temperature ( $T$ ) of electrochemical cells: 1–4 correspond to alloys  $D$  of the phase regions (I)–(IV)

HgSe–Hg<sub>2</sub>GeSe<sub>3</sub>–Ag<sub>2</sub>Hg<sub>3</sub>GeSe<sub>6</sub> (II), GeSe<sub>2</sub>–Hg<sub>2</sub>GeSe<sub>4</sub>–Se–Ag<sub>1.4</sub>Hg<sub>1.3</sub>GeSe<sub>6</sub> (III), and Hg<sub>2</sub>GeSe<sub>4</sub>–Ag<sub>1.4</sub>Hg<sub>1.3</sub>GeSe<sub>6</sub>–Ag<sub>2</sub>Hg<sub>3</sub>GeSe<sub>6</sub>–Hg<sub>2</sub>GeSe<sub>3</sub> (IV). The positions of the lines of two-phase equilibria were determined in Refs. [2, 6–8] and confirmed by our investigations. The spatial position of phase regions (I)–(IV) relative to the figurative point of silver allows us to apply the EMF method to determine the thermodynamic properties of involved ternary and quaternary phases [14]. The positive electrodes  $D$  were prepared by melting the mixture of elements taken in atomic ratio Ag/Hg/Ge/Se = 1.5/3/1/6, phase region (I); 1.5/5/2/9, region (II); 1.1/1.3/1/6, region (III), and 2.4/10.2/5.1/20.4, region (IV).

In accordance with Fig. 1, the virtual electrochemical reactions in the ECCs from the alloys  $D$  of regions (I)–(IV) are described by the equations:



Linear dependences  $E$  vs  $T$  in Fig. 2 are observed in the range of 425–455 K and are approximated by the equations:

$$E_1/\text{mV} = (306.238 \pm 0.80464) + (0.16845 \pm 0.00183)T/\text{K} \quad (420 \leq T/\text{K} \leq 460), \quad (5)$$

$$E_2/\text{mV} = (325.6806 \pm 0.30895) + (0.08268 \pm 0.000704)T/\text{K} \quad (422 \leq T/\text{K} \leq 460), \quad (6)$$

$$E_3/\text{mV} = (311.0379 \pm 0.90231) + (0.15206 \pm 0.00205)T/\text{K} \quad (423 \leq T/\text{K} \leq 457), \quad (7)$$

$$E_4/\text{mV} = (294.9613 \pm 0.7310) + (0.16805 \pm 0.00166)T/\text{K} \quad (423 \leq T/\text{K} \leq 463) \quad (8)$$

The deviations from the linear dependences  $E_{1-4}(T)$  below 425 K result from the kinetic hindrances to achieving the equilibrium in ECCs. The non-linearity of  $E_{1-4}(T)$  above 460 K is likely due to the changes in the concentration regions of the existence of the phases. Eqs. (5)–(8) confirm the correctness of the triangulation of the concentration space of the Ag–Hg–Ge–Se system in the vicinity of the studied phases. Under the condition of  $T = \text{const}$ , the phase region more distant from the figurative point of silver is characterized by higher values of EMF [14]. Specifically, at  $T = 430$  K we observe  $E_1 = 378.7$  mV,  $E_2 = 361.2$  mV,  $E_3 = 376.4$  mV, and  $E_4 = 367.2$  mV.

Gibbs energies of reactions (1)–(4) can be calculated from the measured  $E(T)$  relations by using the basic thermodynamic equation:

$$-\Delta_r G_T = n_e F E(T), \quad (9)$$

where  $n_e = 2, 2, 28, 28$  is the number of electrons involved in the reactions (1)–(4), respectively;  $F = 96,485.3 \text{ C} \cdot \text{mol}^{-1}$  is Faraday’s number.

Applying Eq. (9) to reactions (1)–(4), we obtain

$$\Delta_r G_{T,(1)} = \frac{1}{2} \Delta_f G_{T,Ag_2Hg_3GeSe_6} - \frac{1}{2} \Delta_f G_{T,Hg_2GeSe_4} - \frac{1}{2} \Delta_f G_{T,HgSe}, \quad (10)$$

$$\Delta_r G_{T,(2)} = \frac{1}{2} \Delta_f G_{T,Ag_2Hg_3GeSe_6} + \frac{1}{2} \Delta_f G_{T,Hg_2GeSe_3} - \Delta_f G_{T,Hg_2GeSe_4} - \frac{1}{2} \Delta_f G_{T,HgSe}, \quad (11)$$

$$\Delta_r G_{T,(3)} = \frac{2}{2.8} \Delta_f G_{T,Ag_{1.4}Hg_{1.3}GeSe_6} - \frac{0.7}{2.8} \Delta_f G_{T,GeSe_2} - \frac{1.3}{2.8} \Delta_f G_{T,Hg_2GeSe_4}, \quad (12)$$

$$\Delta_r G_{T,(4)} = \frac{1}{2.8} \Delta_f G_{T,Ag_{1.4}Hg_{1.3}GeSe_6} + \frac{0.7}{2.8} \Delta_f G_{T,Ag_2Hg_3GeSe_6} + \frac{3.4}{2.8} \Delta_f G_{T,Hg_2GeSe_3} - \frac{5.1}{2.8} \Delta_f G_{T,Hg_2GeSe_4}, \quad (13)$$

where  $\Delta_f G_{T, \text{GeSe}_2, \text{HgSe}, \text{Hg}_2\text{GeSe}_3, \text{Hg}_2\text{GeSe}_4,$

**Table 1** Standard thermodynamic properties of saturated solid solutions of compounds in the Ag–Hg–Ge–Se system

Phase	$-\Delta_f G_{298}^{\circ}$ (kJ mol <sup>-1</sup> )	$-\Delta_f H_{298}^{\circ}$ (kJ mol <sup>-1</sup> )	$-\Delta_r S_{298}^{\circ}$ (J mol <sup>-1</sup> K <sup>-1</sup> )	$-T \Delta_r S_{298}^{\circ}$ (kJ mol <sup>-1</sup> )
Hg <sub>2</sub> GeSe <sub>3</sub> (Ag) <sup>a</sup>	30.4 ± 3.0	151.2 ± 2.9	405.3 ± 0.6	120.8 ± 0.2
Hg <sub>2</sub> GeSe <sub>4</sub> (Ag) <sup>a</sup>	30.4 ± 2.8	146.3 ± 2.3	388.8 ± 5.3	115.9 ± 1.6
Ag <sub>2</sub> Hg <sub>3</sub> GeSe <sub>6</sub>	139.4 ± 3.3	247.8 ± 2.9	363.6 ± 5.4	108.3 ± 1.6
Ag <sub>1.4</sub> Hg <sub>1.3</sub> GeSe <sub>6</sub>	90.2 ± 2.3	173.1 ± 2.0	278.0 ± 3.8	82.8 ± 1.2

<sup>a</sup> Phases saturated by silver

Ag<sub>1.4</sub>Hg<sub>1.3</sub>GeSe<sub>6</sub>, Ag<sub>2</sub>Hg<sub>3</sub>GeSe<sub>6</sub> are Gibbs energies of the formation of the appropriate phases from the elements at specified temperature  $T$ . In the approximation of small differences of the values of the thermodynamic func-

tions of saturated solid solutions of the compounds in bordering phase regions, Eqs. (10)–(13) form a system of linear equations, from which the resulting  $\Delta_f G_T$  were obtained as

$$\Delta_f G_{T, \text{Hg}_2\text{GeSe}_4} = -\frac{132}{7} \Delta_r G_{T, (1)} + \frac{136}{7} \Delta_r G_{T, (2)} + 4 \Delta_r G_{T, (3)} - 8 \Delta_r G_{T, (4)} + 2 \Delta_f G_{T, \text{HgSe}} + \Delta_f G_{T, \text{GeSe}_2}, \quad (14)$$

$$\Delta_f G_{T, \text{Hg}_2\text{GeSe}_3} = \Delta_f G_{T, \text{Hg}_2\text{GeSe}_4} + 2(\Delta_r G_{T, (2)} - \Delta_r G_{T, (1)}), \quad (15)$$

$$\Delta_f G_{T, \text{Ag}_2\text{Hg}_3\text{GeSe}_6} = 2 \Delta_r G_{T, (1)} + \Delta_f G_{T, \text{Hg}_2\text{GeSe}_4} + \Delta_f G_{T, \text{HgSe}}, \quad (16)$$

$$\Delta_f G_{T, \text{Ag}_{1.4}\text{Hg}_{1.3}\text{GeSe}_6} = 1.4 \Delta_r G_{T, (3)} + 0.35 \Delta_f G_{T, \text{GeSe}_2} + 0.65 \Delta_f G_{T, \text{Hg}_2\text{GeSe}_4} \quad (17)$$

Taking into account Eq. (9),  $\Delta_f G_{T, \text{HgSe}} / (\text{kJ mol}^{-1}) = (-43.52 \pm 0.05) + (17.33 \pm 0.05) \times 10^{-3} T / \text{K}$  ( $298 \leq T / \text{K} \leq 450$ ) [15] and  $\Delta_f G_{T, \text{GeSe}_2} / (\text{kJ mol}^{-1}) = (-102.6 \pm 1.2) + (130.8 \pm 3.5) \times 10^{-3} T / \text{K}$  ( $298 \leq T / \text{K} \leq 535$ ) [13], Eqs. (14)–(17) result in:

$$\Delta_f G_{T, \text{Hg}_2\text{GeSe}_4} / (\text{kJ mol}^{-1}) = (-146.3 \pm 2.3) + (388.8 \pm 5.3) \times 10^{-3} T / \text{K} \quad (420 \leq T / \text{K} \leq 460), \quad (18)$$

$$\Delta_f G_{T, \text{Hg}_2\text{GeSe}_3} / (\text{kJ mol}^{-1}) = (-151.2 \pm 2.9) + (405.3 \pm 0.6) \times 10^{-3} T / \text{K} \quad (422 \leq T / \text{K} \leq 460), \quad (19)$$

$$\Delta_f G_{T, \text{Ag}_2\text{Hg}_3\text{GeSe}_6} / (\text{kJ mol}^{-1}) = (-247.8 \pm 2.9) + (363.6 \pm 5.4) \times 10^{-3} T / \text{K} \quad (423 \leq T / \text{K} \leq 457), \quad (20)$$

$$\Delta_f G_{T, \text{Ag}_{1.4}\text{Hg}_{1.3}\text{GeSe}_6} / (\text{kJ mol}^{-1}) = (-173.1 \pm 2.0) + (278.0 \pm 3.8) \times 10^{-3} T / \text{K} \quad (423 \leq T / \text{K} \leq 463) \quad (21)$$

Equations (18)–(21) express the temperature dependence of Gibbs energy of the formation of saturated solid solutions of corresponding phases from their elements. The values of the standard thermodynamic functions of phases calculated according to Eqs. (18)–(21) in the approximation  $\Delta C_p = 0$  [27], are listed in Table 1. The values of entropy factor  $T \Delta_r S_{298}^{\circ}$  and enthalpy factor  $\Delta H_{298}^{\circ}$  are listed for the comparison of their contribution to  $\Delta G_{298}^{\circ}$ . High negative values of  $\Delta_r S_{298}^{\circ}$  indicate the decrease of the grain dispersion and the increase of the symmetry of the crystal lattice of ternary and quaternary compounds upon the formation of solid solutions.

## Conclusions

1. The equations of the temperature dependence of Gibbs energy of the formation of saturated solid solutions of Hg<sub>2</sub>GeSe<sub>3</sub>, Hg<sub>2</sub>GeSe<sub>4</sub>, Ag<sub>2</sub>Hg<sub>3</sub>GeSe<sub>6</sub>, and Ag<sub>1.4</sub>Hg<sub>1.3</sub>GeSe<sub>6</sub> compounds were obtained by EMF method.
2. The standard thermodynamic properties of the listed compounds were calculated in the approximation  $\Delta C_p = 0$ .
3. The formation of solid solutions of ternary and quaternary compounds is accompanied by the decrease of the grain

dispersion and the increase of the symmetry of the crystal lattice as indicated by high negative values of  $\Delta_r S_{298}^0$ .

- The calculated values of the standard thermodynamic functions of the phases can be used in modeling the  $p$ – $T$ – $x$  diagrams of the Ag–Hg–Ge–Se system by CALPHAD methods.

## References

- Hansen M, Anderco K (1958) Constitution of binary diagram. MacGraw–Hill, New York
- Novoselova AV, Zlomanov VP, Karbanov SG, Matveyev OV, Gas'kov AM (1972) Physico-chemical study of the germanium, tin, lead chalcogenides. *Prog Solid State Chem* 7:85–115
- Salaeva ZY, Allazov MR, Movsum-zade AA (1985) The system  $\text{Ag}_2\text{Se}$ – $\text{GeSe}_2$  and  $\text{Ag}_8\text{GeSe}_6$ – $\text{Ge}$ . *Zh Neorg Khim* 30:1834–1837
- Gorochov O (1968) Les composés  $\text{Ag}_8\text{MX}_6$  ( $\text{M} = \text{Si}, \text{Ge}, \text{Sn}$  et  $\text{X} = \text{S}, \text{Se}, \text{Te}$ ). *Bull Soc Chim France* 6:2263–2265
- Borisova ZU, Rykova TS, Turkina EY, Tabolin AR (1984) Phase relations and glass formation in the Ge–Se–Ag system. *Neorg Mater* 20:1796–1798 [in Russian]
- Motria SF (1991) Mercury–germanium(tin)–sulfur(selenium) ternary systems. In: Yu V (ed) *Poluchenie i svoistva slozhnykh poluprovodnikov*. Umkvo, Kiev, pp. 17–26 [in Russian]
- Tomashyk V, Feychuk P, Shcherbak L (2013) Ternary alloys based on II–VI semiconductor compounds. Taylor & Francis, London
- Parasyuk OV, Gulay LD, Romanyuk YE, Olekseyuk ID, Piskach LV (2003) The  $\text{Ag}_2\text{Se}$ – $\text{HgSe}$ – $\text{GeSe}_2$  system and crystal structures of the compounds. *J Alloys Compd* 351:135–144
- Dong Y, Kim S, Yun H (2005) Reinvestigation of  $\text{Hg}_2\text{GeSe}_4$  based on single-crystal data. *Acta Crystallogr Sect E: Struct Rep Online* 61(2):i9–i11
- Gulay LD, Olekseyuk ID, Parasyuk OV (2002) Crystal structures of the  $\text{Ag}_6\text{HgGeSe}_6$  and  $\text{Ag}_6\text{HgSiSe}_6$  compounds. *J Alloys Compd* 343:116–121
- Voronin MV, Osadchii EG (2011) Determination of thermodynamic properties of silver selenide by the galvanic cell method with solid and liquid electrolytes. *Russ J Electrochem* 47:420–426
- Feng D, Taskinen P, Tesfaye F (2013) Thermodynamic stability of  $\text{Ag}_2\text{Se}$  from 350 to 500K by a solid state galvanic cell. *Solid State Ionics* 231:1–4
- Moroz MV, Prokhorenko MV (2015) Determination of thermodynamic properties of saturated solid solutions of the Ag–Ge–Se system using EMF technique. *Russ J Electrochem* 51:697–702
- Babanly M, Yusibov Y, Babanly N (2011) The EMF method with solid-state electrolyte in the thermodynamic investigation of ternary copper and silver chalcogenides. In: Sadik Kara (ed) *Electromotive force and measurement in several systems*. InTech. doi:10.5772/2109
- Barin I (1995) Thermochemical data of pure substance. VCH, Weinheim
- Ipser H, Mikula A, Katayama I (2010) Overview: the emf method as a source of experimental thermodynamic data. *Calphad* 34:271–278
- Kroupa A (2013) Modelling of phase diagrams and thermodynamic properties using Calphad method—development of thermodynamic databases. *Comput Mater Sci* 66:3–13
- Parasyuk OV, Gulay LD, Romanyuk YE, Olekseyuk ID (2003) The  $\text{Ag}_2\text{Se}$ – $\text{HgSe}$ – $\text{SiSe}_2$  system in the 0–60 mol.%  $\text{SiSe}_2$  region. *J Alloys Compd* 348:157–166
- Robinel E, Kone A, Duclot MJ, Souquet JL (1983) Silver sulfide based glasses:(II). Electrochemical properties of  $\text{GeS}_2$ – $\text{Ag}_2\text{S}$ – $\text{AgI}$  glasses: transference number measurement and redox stability range. *J Non-Cryst Solids* 57:59–70
- Preston-Thomas H (1990) The international temperature scale of 1990 (ITS-90). *Metrologia* 27:3–10
- Diffractionmeter Stoe WinX<sup>POW</sup>, version 2.21, Stoe & Cie GmbH, Darmstadt, 2007
- Kraus W, Nolze G (1999) Cell for windows (version 2.3). Federal Institute for Materials Research and Testing, Berlin
- Moroz MV, Demchenko PY, Mykolaychuk OG, Akselrud LG, Gladyshevskii RE (2013) Synthesis and electrical conductivity of crystalline and glassy alloys in the  $\text{Ag}_3\text{GeS}_3\text{Br}$ – $\text{GeSe}_2$  system. *Inorg Mater* 49:867–871
- West AR (2014) Solid state chemistry and its applications. John Wiley & Sons
- Tesfaye F, Taskinen P, Aspiala M, Feng D (2013) Experimental thermodynamic study of intermetallic phases in the binary Ag–Te system by an improved EMF method. *Intermetallics* 34:56–62
- Osadchii EG, Echmaeva EA (2007) The system Ag–Au–Se: phase relations below 405 K and determination of standard thermodynamic properties of selenides by solid-state galvanic cell technique. *Am Mineral* 92:640–647
- Swalin RS (1972) Thermodynamics of solids. John Wiley & Sons